Heliyon 5 (2019) e02240

Contents lists available at ScienceDirect

Heliyon

journal homepage: www.heliyon.com

The proton conductivity and mechanical properties of Nafion®/ ZrP nanocomposite membrane

R. Sigwadi [a,*], M.S. Dhlamini [b], T. Mokrani [a], F. Ṇemavhola [e], P.F. Nonjola [c], P.F. Msomi [d]

[a] Department of Chemical Engineering, University of South Africa, Private Bag X6, Florida, 1710, South Africa
[b] Department of Physics, University of South Africa, Private Bag X6, Florida, 1710, South Africa
[c] CSIR (Energy Centre), PO BOX 395, Pretoria, 0001, South Africa
[d] Department of Applied Chemistry, University of Johannesburg, Johannesburg, South Africa
[e] Department of Mechanical and Industrial Engineering, University of South Africa, Private Bag X6, Florida, 1710, South Africa

ARTICLE INFO

Keywords:
Materials science
Nanotechnology
Nanomaterials
Coatings
Metals
Materials class
Computational materials science
Materials application
Degradation
Impregnating
Zirconium phosphates
Proton conductivity
Water uptake
Methanol permeability

ABSTRACT

Zirconium phosphates (ZrP) were incorporated into Nafion® 117 membrane by impregnating method to obtain a reduced methanol permeation and improved proton conductivity for fuel cell application. The mechanical properties and water uptake of Nafion® membrane incorporated with zirconium phosphates nanoparticles was more improvement when compared to the commercial Nafion® 117, due to the presence of phosphoric acid within the nanoparticles. The effect of ZrP nano filler on the membrane structural morphology and thermal properties were investigated by Fourier-transform infrared spectroscopy (FTIR), X-ray diffraction (XRD), Thermal gravimetric analysis (TGA) and Scanning Electron Microscopy (SEM). The improved ion conductivity and decreased methanol permeability on the nanocomposite membranes showed a great potential for fuel cell applications. The nanocomposite membrane with high tensile strength was obtained due to the well dispersed zirconium phosphates within the Nafion® matrix.

1. Introduction

Fuel cell is an electrochemical device, which directly converts chemical energy into an electrical energy by using various fuels such as methanol, hydrogen, natural gas, ethanol, glucose and methylene blue in a reaction with an oxidant (oxygen). The direct methanol fuel cells (DMFCs) only utilise methanol as fuel. Nafion® membranes have high proton conductivity, mechanical and chemical stability in its hydrated state and lower temperature, which make them a promising fuel cell electrolyte for transport, portable and stationary application [1, 2]. However, at high temperature and low relative humidity, Nafion® membranes faces some challenges of higher permeation of methanol and dramatically drops of protons conduction due to their dependence on hydration [3]. The researches prompt a research on the reduction of methanol crossover and improves the fuel cell performance by incorporation of nanometre-sized particles of hygroscopic inorganic acids or oxides, which act as a water reservoir into the polymer matrix. This hygroscopic inorganic acids such as zirconium phosphate (ZrP) has been used to modify the Nafion® membrane due to their hydrophilic nature, proton conducting material, very low in toxic, inexpensive, not soluble in water and stable in a hydrogen/oxygen atmosphere [4, 5]. Modified Nafion® membrane with ZrP nanofiller found to have a reduced methanol permeability and enhanced proton conductivity due to good water retention capabilities and high proton mobility on the surface of ZrP particles while maintaining high power density [6, 7]. Costamagna et al obtained stable behaviour on Nafion®/zirconium phosphate membranes with the electronic current of 1500 mA/cm^2 while compared with Nafion® membrane that sustain an irreversible degradation with the electronic current of 250 mA/cm^2 produced at 0.45 V and 130 °C temperature [8, 9]. Similarly, Alberti et al obtained the higher conductivity at 140 °C and 90% relative humidity when modified Nafion® membrane with 10wt% zirconium phosphate when compare to pure recast Nafion® membrane [7, 10]. Moreover, the modified Nafion® membrane with ZrP obtained a decreased methanol permeability at 150 °C while preserving

* Corresponding author.
E-mail address: masitfj@unisa.ac.za (R. Sigwadi).

https://doi.org/10.1016/j.heliyon.2019.e02240
Received 4 December 2018; Received in revised form 8 June 2019; Accepted 2 August 2019

the water content and proton conductivity [11]. Nanocomposite membranes shows an improvement on the tensile modulus, stiffness and exhibit better fuel cell performance than pure Nafion® 117 membrane under high temperature and low RH conditions [6]. The purpose of this work was to synthesis the modified Nafion® 117 membrane by acidic zirconia that may reduce the methanol crossover while improving the water uptake, proton conductivity and mechanical strength of membrane. The stress-strain of Nafion® 117 membrane and Nafion®/ZrP nanocomposite membrane were recorded.

2. Experimental

2.1. Materials

Phosphoric acid (Sigma), Zirconium oxychloride hydrate (Merck), Sulfuric acid (Merck), Nafion® 117 membrane (Sigma), Methanol (sigma) and hydrogen peroxide (Merck) were used as received.

2.2. Zirconia phosphates preparation (ZrP)

The zirconia phosphates (ZrP) nanoparticles was synthesised by adding 120 mL of 0.4 M $ZrOCl_2{\cdot}8H_2O$ aqueous solution in 6 M solution of phosphoric acid (H_3PO_4) and stirred for 30 min. The solution was then refluxed at 80 °C for further 24 h while stirring. The obtained material was then centrifuged and washed extensively with distilled water up to pH 3 and dried at 80 °C and then calcinated it at 600 °C for 2 h.

2.3. Synthesis of nanocomposite membranes (impregnation method)

Purification of Nafion® 117 membranes were done by boiling in hydrogen peroxide (3% solution) for 1hr, then boiled in sulfuric acid (0.5 M) and finally boiled in distilled water [12]. The nanocomposite membranes were pre-soaked in the methanol solution and 2.5wt %, 5wt % and 7.5wt % of ZrP nanoparticles were added. The soaking procedure of the membrane were repeated five times [13], and then heated at 100 °C for 2 h. The remaining solution were kept at room temperature for 24 h. The digital micrometre were used to measure the membranes thicknesses (0.18 mm). The thickness reading was taken more than 2 times in order to record the exact number.

2.4. Characterisations

The characterisations of membranes were observed under thermal gravimetric analysis (TGA), X-ray diffraction (XRD) analysis, Scanning Electron Microscopy (SEM) and Fourier-transform infrared spectroscopy (FTIR).

2.5. Tensile test

The mechanical strength of membranes was observed under uniaxial testing system. The Vernier caliper was used to measure the width, thickness and length. The 4 mm × 10 mm dimension were used in all the membranes, in order to allow the clamping area. The observed thickness of 0.18 mm was used to calculate the stress applied to the sample. The CellScale Ustretch device were used to measure membranes at 25 °C at the actuator speed of 50, 40, 30, 20 and 10 mm/min.

2.6. Water uptake ((WU)) and swelling ratio (SR)

The distilled water was used to soak membranes at the temperature of 30 °C, 60 °C and 80 °C for 24 h. After soaking the membranes was weighed in order to calculate water uptake and measured in order to calculate swelling ratio using the equations below:

$$W_{up} = \frac{(m_{wet} - m_{dry})}{m_{dry}} x100\ \% \quad (1)$$

$$SR = \frac{(L_w - L_d)}{L_d} x\ 100\ \% \quad (2)$$

Where W_{up} is the WU percentage, m_{wet}, membrane wet mass and m_{dry}, membrane driy mass, L_w membrane wet length and L_d dried length of membrane.

2.7. Ion exchange capacity (IEC)

The IEC of membranes were calculated from the titrated results and calculated using the equation below:

$$IEC = \frac{V_{NaOH} \times C_{NaOH}}{m_d} \quad (3)$$

Where m_d is the membrane dried mass and V_{NaOH} is the volume of titrated NaOH.

2.8. Measurements of the methanol permeability

The methanol crossover was measured with a permeation-measuring cell designed in our lab that consisted of two compartments. Compartments (A) filled with methanol solution (50 mL) and compartment (B) filled with distilled water (50 mL). The membrane was mounted between the two compartments with a diffusion area diameter of 3.5 cm. The 5M and 2M methanol solutions were used and the reading were taken at 30 °C, 60 °C and 80 °C. Methanol permeability (P) was calculated using the below equation:

$$C_B = \frac{A\,P}{V_B\,L}\ C_A\ (t - t_o) \quad (4)$$

where $C_B(t)$ the concentration of methanol in compartment B at diffusion time t; C_A is the concentration of methanol in compartment A; V_B the distilled water volume in compartment B; L the membrane thickness; and A is the effective permeating area.

2.9. Measurement of the proton conductivity

The membranes conductivities were measured using a four-point probe conductivity cell at 30 °C and 60 °C under 70% relative humidity (RH). The proton conductivity was observed galvanostatically at 0.1 mA current and 1MHz to 10Hz frequencies and calculated using the equation below:

$$\sigma = \frac{L}{AR_s} \quad (5)$$

where R_s is the membrane resistance obtained, A is the membrane area normal to the current flow and L is the membrane thickness.

2.10. The cell polarization and the fabrication of membrane electrode assembly

The direct methanol fuel cell (DMFC) was used to evaluate the membranes performance. The membrane electrode assembly (MEA) of anode and the cathode were consists of Pt on carbon cloth, which have been ordered from Fuel cell Store. The MEA was assembled without hot pressing. The methanol solution of 2 M was used in fuel cell testing at 60 °C. The fuel cell potential was measured galvanostatically in open air on a single fuel cell test.

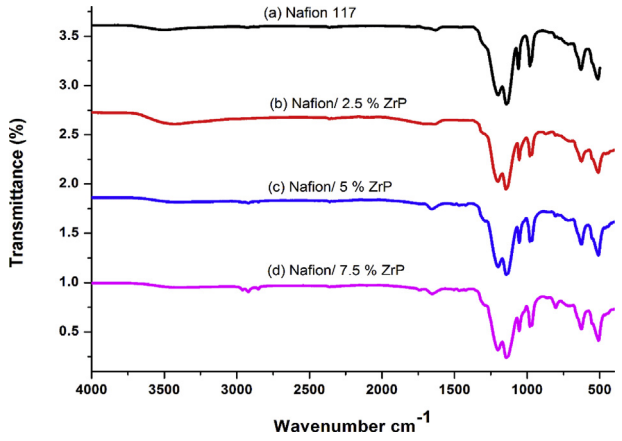

Fig. 1. FTIR spectra of (a) Nafion® 117 membrane, (b) Nafion®/2.5% ZrP, (c) Nafion®/5% ZrP and (d) Nafion®/7.5% ZrP nanocomposite membranes.

3. Results and discussion

3.1. Fourier transform infrared

Fig. 1 shows the spectra of Nafion® 117 membrane and modified Nafion® membranes in the range of 400–4000 cm^{-1}. Fig. 1(a-d) shows the O–H stretching vibration at 3456 cm^{-1}, corresponding to physically adsorbed water [3, 14] and 1630 cm^{-1} attributed to O–H bending vibration of free water molecules. Fig. 1(c & d) shows the peaks at 3456 cm^{-1} is less shallow than commercial membrane. These can be due to the impregnated ZrP, which enhance the water content within the Nafion®/ZrP nanocomposite membranes. The nanocomposite membrane and commercial membrane have the peak at 1060 cm^{-1}, due to symmetric S–O stretching [15, 16], the band at 1145 cm^{-1}, due to symmetric C–F stretching and a band at 1201 cm^{-1}, due to asymmetric C–F stretching [17]. Moreover, the peaks observed at 976 cm^{-1} attributed to the C–O–C stretching [17], the band at 512 cm^{-1} is attributed to symmetric O–S–O bending and the band at 632 cm^{-1} is assigned to the stretching of C–S groups [17, 18]. Furthermore, Nafion®/ZrP nanocomposite membranes shows that the ZrP nanoparticles was successfully impregnated, as the FTIR spectra peaks of Zr–O and P–O_4 are identified at 797 cm^{-1}, 509 cm^{-1} and 446 cm^{-1} [19,20]. Fig. 1(d) also present the band at 1016 cm^{-1} and 1550 cm^{-1}, which are attributed to bending vibrations of Zr–OH showing that zirconia nanoparticles was successfully impregnated within the nanocomposite membrane [21]. The stretch vibrations between 2925 and 2865 cm^{-1} increases with the increase of ZrP nanoparticles, which are attributed to the C–H stretching of the modified Nafion® membrane as presented in Fig. 1(b-d) [22].

3.2. Scanning Electron Microscopy (SEM)

Fig. 2 shows SEM surface morphologies of the Nafion®/ZrP nanocomposite and Nafion® 117 membranes. Fig. 2(a) shows the plain Nafion® 117 membrane, which is dark in colour without nanoparticles. This SEM image in Fig. 2(b) shows that ZrP nanoparticles within the membrane are uniform in shape and well distributed within the membrane matrix. When 5% of ZrP is added in Nafion membrane, the nanoparticle is well distributed as shown in Fig. 2(c). The SEM image of Nafion®/7.5% ZrP nanocomposite membrane in Fig. 2(d) shows ZrP nanoparticles are agglomerated. In conclusion, the results show that, when less than 5% ZrP nanoparticles been used as nanofiller, ZrP is well

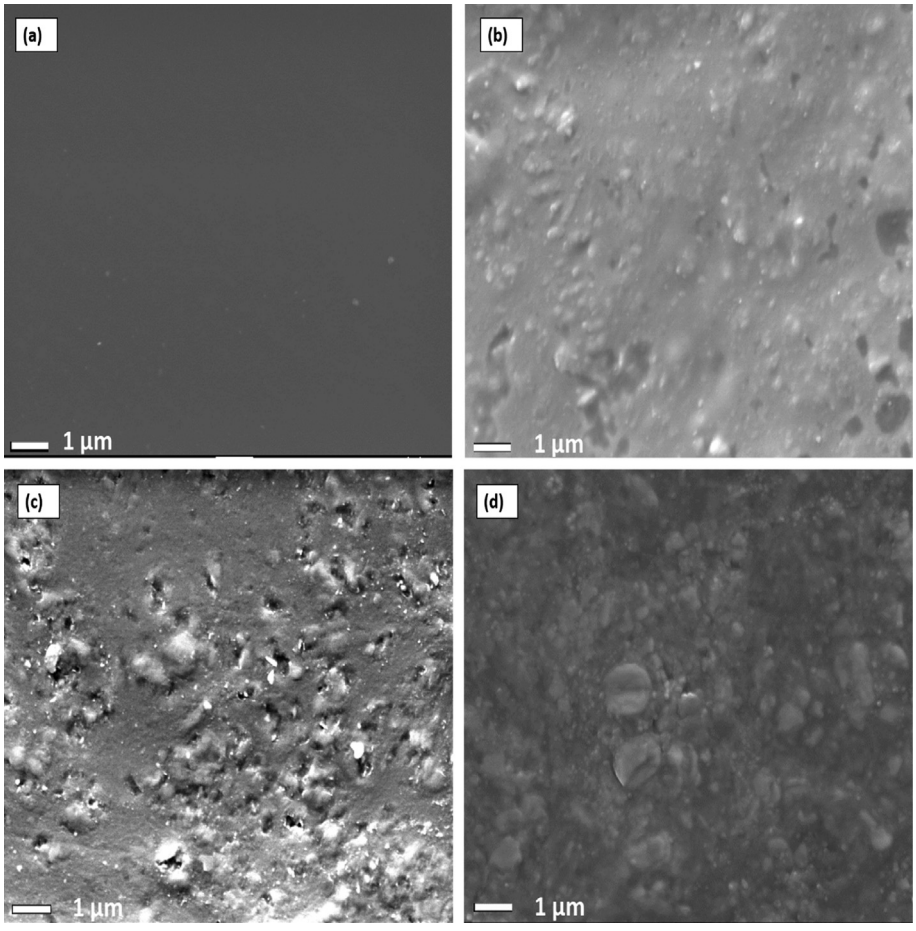

Fig. 2. SEM micrograph of (a) of Nafion® 117 membrane, (b) Nafion®/2.5% ZrP, (c) Nafion®/5% ZrP and (d) Nafion®/7.5% ZrP nanocomposite membranes.

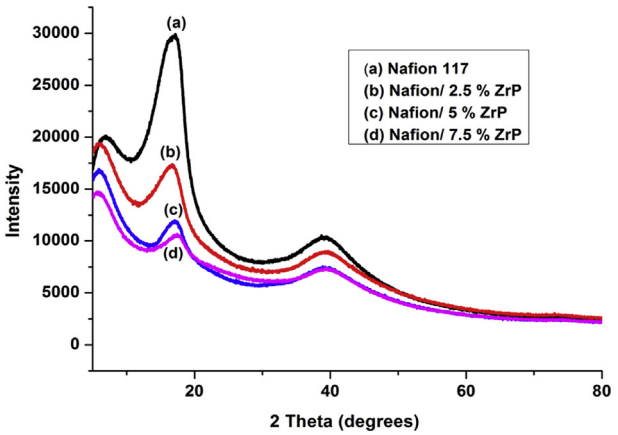

Fig. 3. XRD patterns of (a) of Nafion® 117 membrane, (b) Nafion®/2.5% ZrP, (c) Nafion®/5% ZrP and (d) Nafion®/7.5% ZrP nanocomposite membranes.

distributed within the membrane matrix and less agglomerated.

3.3. Structure analysis

Fig. 3 shows the XRD results of modified Nafion® 117 and nanocomposite membranes. Nafion® 117 membrane shows only two diffraction peaks at 17.5° and 39° 2θ as shown in Fig. 3(a), which can be attributed to semi crystalline of the perfluorocarbon chains of the ionomer [23]. The composited membranes with ZrP shows a little effect on the crystallinity, but with the lower peak height as shown in Fig. 3(b-d). Nevertheless, the incorporation of ZrP in Nafion® membrane resulted on amorphous shape and the slightly shift of 17 °peak compared to the commercial membrane, as confirmed by TGA results [24]. Moreover, when ZrP weight % increase from 2.5 to 7.5 it lowers the crystallinity and the modified membrane become more amorphous.

3.4. Thermo-gravimetric analysis (TGA)

The TGA and derivative thermogravimetric (DTG) of commercial Nafion® 117 and nanocomposite membranes are shown in Fig. 4. In Fig. 4, it was observed that the membrane undergoes three weight-loss stages. At lower temperature of 100 °C the commercial Nafion® 117 membrane initial lose weight, which corresponding to the adsorption of water bonded to the sulfonic groups as shown in Fig. 4 [25]. The second weight loss starts at 380 °C, due to the sulfonic groups degradation [26]. The third weight loss was assigned to degradation of the polymer backbone chain [27]. However, Nafion®/7.5 wt% ZrP nanocomposite membrane initial lose weight at 150 °C that corresponds to the water adsorption. The second weight loss at 490 °C is due to the decomposition of the sulfonic acid groups [26]. The modified Nafion®/7.5 wt% ZrP membrane showed improved thermal degradation at high temperature of 490 °C that may be due to the nature of inorganic filler and their close interaction with the hydrophobic Nafion® backbone whereas the commercial Nafion® 117 initially decomposed at 380 °C [28]. The final weight loss around 700–900 °C was due the polymer main chain degradation [27], with 7.5% residue remain. The Nafion®/7.5%wt ZrP, Nafion®/5%wt ZrP and Nafion®/2.5%wt ZrP nanocomposite membranes showed thermal stability up to 340 whereas Nafion® 117 membrane showed a thermal stability up to 240 (DTG insert) in Fig. 4. This may be due to the water retention nanoparticles incorporated in Nafion® membrane [29], which make the suitable used in fuel cell applications. Fig. 4 (insert) showed two decomposition peaks in Nafion® and modified membranes. Fig. 4 (insert) shows that the modified Nafion® membrane with 7.5% ZrP nanoparticle obtained the highest thermal stability compared to Nafion® 117 membrane.

3.5. Tensile tests

Fig. 5 shows the stress-strain curves of the commercial Nafion® 117 membrane compared with Nafion®/2.5% ZrP, Nafion®/5% ZrP and Nafion®/7.5% ZrP nanocomposite membrane at 50, 40, 30, 20 and 10 mm/min. The stress rate of 50, 40, 30 mm/min, 20 and 10 mm/min show the elasticity and flexibility of the commercial Nafion® membrane at 0.6 stress versus strain as shown in Fig. 5(a). Fig. 5(b-c) shows that when increasing the strain rate to 50 mm/min decreases the tensile stress, whereas when the strain rate decreases to 30 mm/min increasing the

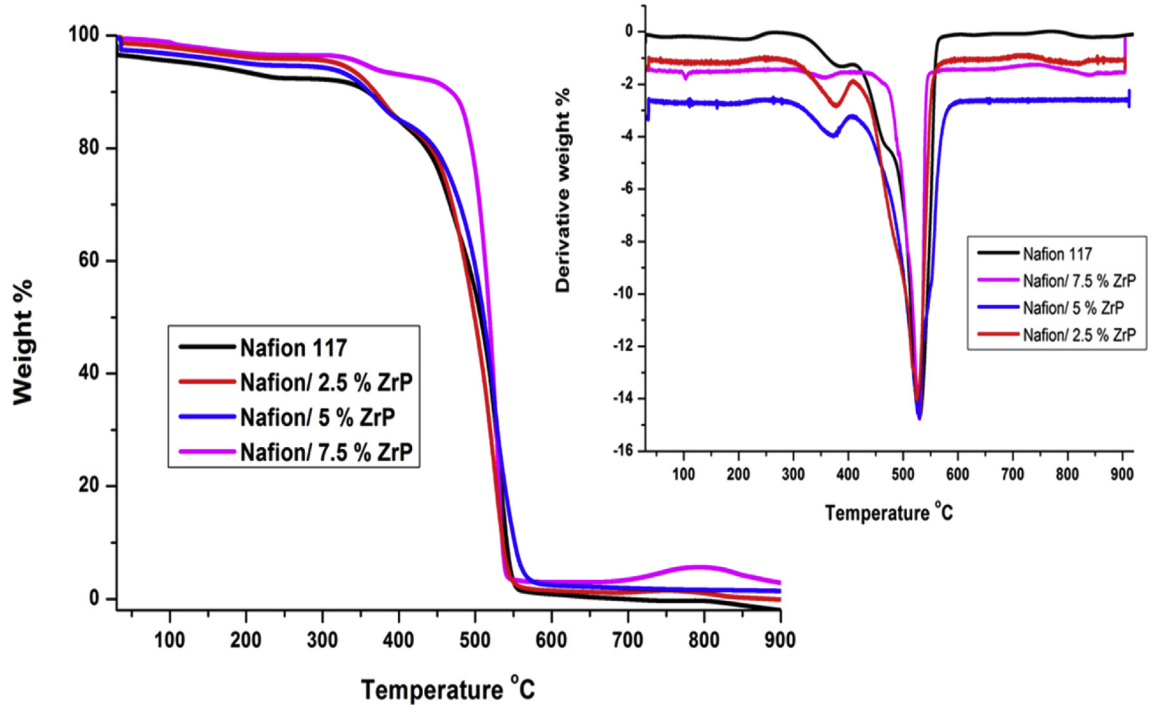

Fig. 4. The TGA and DTG of (a) Nafion® 117 membrane, (b) Nafion®/2.5% ZrP, (c) Nafion®/5% ZrP, (d) Nafion®/7.5% ZrP nanocomposite membranes.

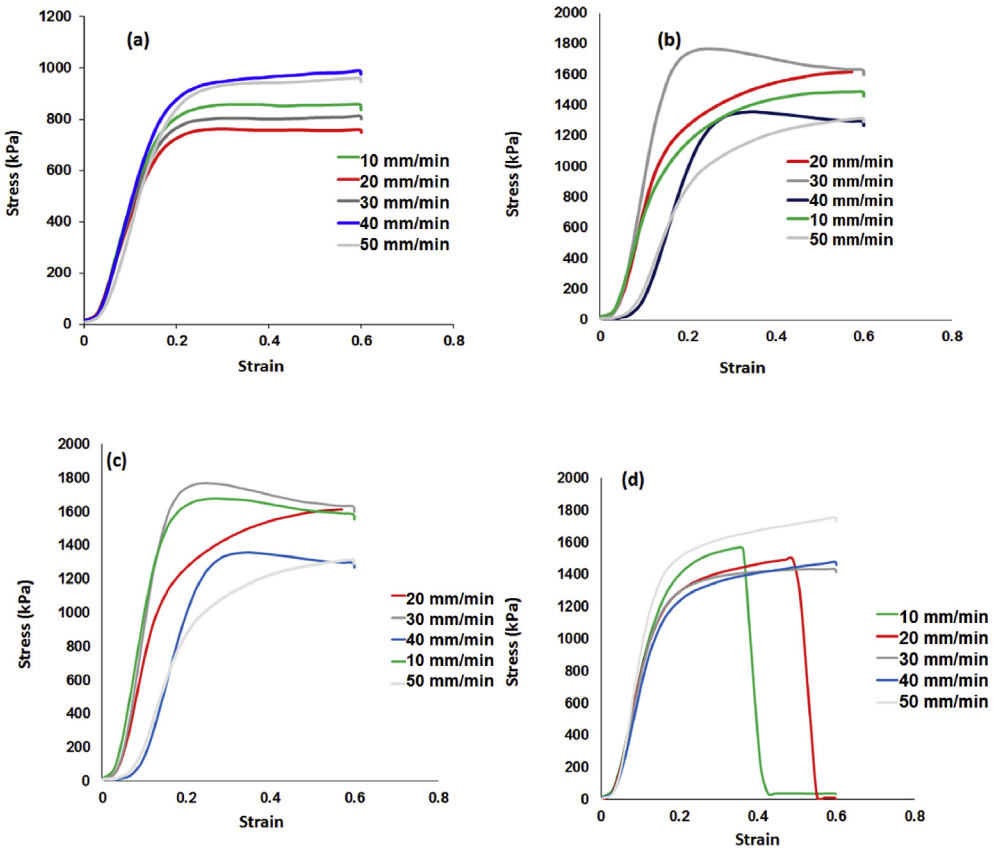

Fig. 5. Mechanical tensile tests results of (a) Nafion® 117 membrane, (b) Nafion®/2.5% ZrP, (c) Nafion®/5% ZrP and (d) Nafion®/7.5% ZrP nanocomposite membranes shows stress versus strain ratio curve.

tensile stress to 1737 kPa and 1790 kPa, respectively, this may due to the percentage of ZrP nanoparticles deposited in the membrane. The stress-strain of 10 mm/min, 20 mm/min and 40 mm/min were merely affected by varying the strain rate values, as there was no difference on their tensile strain. The engineering stress and strain were presented in the form of the graph as shown in Fig. 5. The strain rate used for testing the maximum allowable stress for Nafion® varies widely from 0.08 mm/min to 50 m/s [30, 31, 32]. Furthermore, the stress-strain of the Nafion®/7.5 ZrP were higher than Nafion® 117 membrane at a strain rate of 50 mm/min were 1737 kPa and 947 kPa, respectively as shown in Fig. 5(d). Whereas some of the strain rate of nanocomposites membrane shows a lower strain of 3.7 and 4.9, but with a higher stress than Nafion® 117 membrane. Moreover, the stress-strain of the nanocomposite membrane were higher than Nafion® 117 membrane. Generally, the results showed that the modification of Nafion® membrane with zirconia phosphates has improvement on the stress-strain, which is good

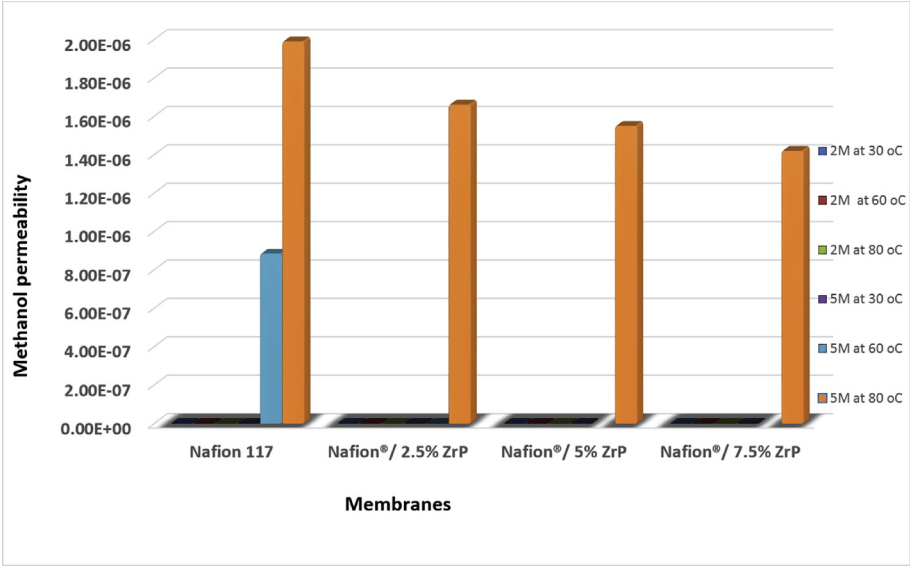

Fig. 6. The methanol permeability of Nafion® 117, Nafion®/2.5% ZrP, Nafion®/5% ZrP and Nafion®/7.5% ZrP nanocomposite membranes at 5M and 2M concentration.

Table 1
The methanol permeability of Nafion® 117 membrane, Nafion®/2.5% ZrP, Nafion®/5% ZrP and Nafion®/7.5% ZrP nanocomposite membranes.

Methanol solutions	2M	2M	2M	5M	5M	5M
Temperature	30 °C	60 °C	80 °C	30 °C	60 °C	80 °C
Nafion 117	-	-	-	-	8.84E-07	1.99E-06
Nafion®/2.5% ZrP	0	0	0	0	0	1.66E-06
Nafion®/5% ZrP	0	0	0	0	0	1.55E-06
Nafion®/7.5% ZrP	0	0	0	0	0	1.42E-06

properties for DMFC [33]. However, the stress-strain of modified membrane with the higher percentage of ZrP nanoparticles in Fig. 5(a), is not compactible for the lower stress rate as it reduces the elasticity and mechanical properties as compared to the commercial Nafion® 117 membrane, which shows the elastic in the entire stress rate as shown. This can be resulted from little agglomeration of ZrP nanoparticles in the Nafion® matric, which introduced the brittle fracture in the modified membrane.

3.6. Methanol permeability

Fig. 6 shows the methanol permeability of Nafion® 117 and modified Nafion® membranes with 2.5% ZrP, 5% ZrP and 7.5% ZrP nanoparticles. The methanol permeability of nanocomposite membrane was lower than that of commercial Nafion® 117; due to ZrP added to Nafion® 117 that improve the barrier properties of Nafion® membrane towards methanol and further illustrated in Table 1. Table 1 lists the methanol permeability measured at different temperatures of 30 °C, 60 °C and 80 °C and methanol concentration of 2 M and 5 M. As observed by Yang *et al.*, the decrease of the methanol concentration can reduce the methanol crossover due to the decreased concentration gradient [34]. Therefore, in this study, a higher concentration of 5 M methanol solution was also used. Fig. 6 shows that the methanol permeability of Nafion® 117 and Nafion®/ZrP nanocomposite membranes measured at 60 °C were 8.84 10^{-7} cm^2/s and 0 cm^2/s (no crossover), respectively. Fig. 6 shows that the methanol permeability of modified and unmodified Nafion® membranes increases as the temperature increases. The results show that Nafion®/ZrP nanocomposite membranes obtain a lower methanol permeation when the temperature rise to 80 °C, which indicate that there is more water permeation at high temperature than methanol. The methanol permeability for Nafion® 117, Nafion®/2.5% ZrP, Nafion®/5% ZrP and Nafion®/7.5% ZrP nanocomposite membranes are 1.99×10^{-6} cm^2/s, 1.66×10^{-6} cm^2/s, 1.55×10^{-6} cm^2/s and 1.42×10^{-6} cm^2/s, respectively as shown in Table 1. As indicated in Table 1, the modified Nafion® membrane with ZrP nanoparticles shows a slight decrease of methanol permeability when compared to Nafion® 117 membrane, due to ZrP that prevent the permeation of methanol in the membranes. The results show that the methanol permeation in the nanocomposite membranes decrease with the amount of ZrP nanoparticles added. Moreover, the modified Nafion® nanocomposite membranes seem to be the promising electrolytes for fuel cell application.

3.7. Water uptake, dimensional swelling ratio, Ion exchange capacity and proton conductivity measurement

The water uptake of Nafion®/2.5%, ZrP Nafion®/5% ZrP, and Nafion®/7.5% ZrP nanocomposite and commercial Nafion® 117 membranes are shown in Fig. 7(a). The test method was described in section

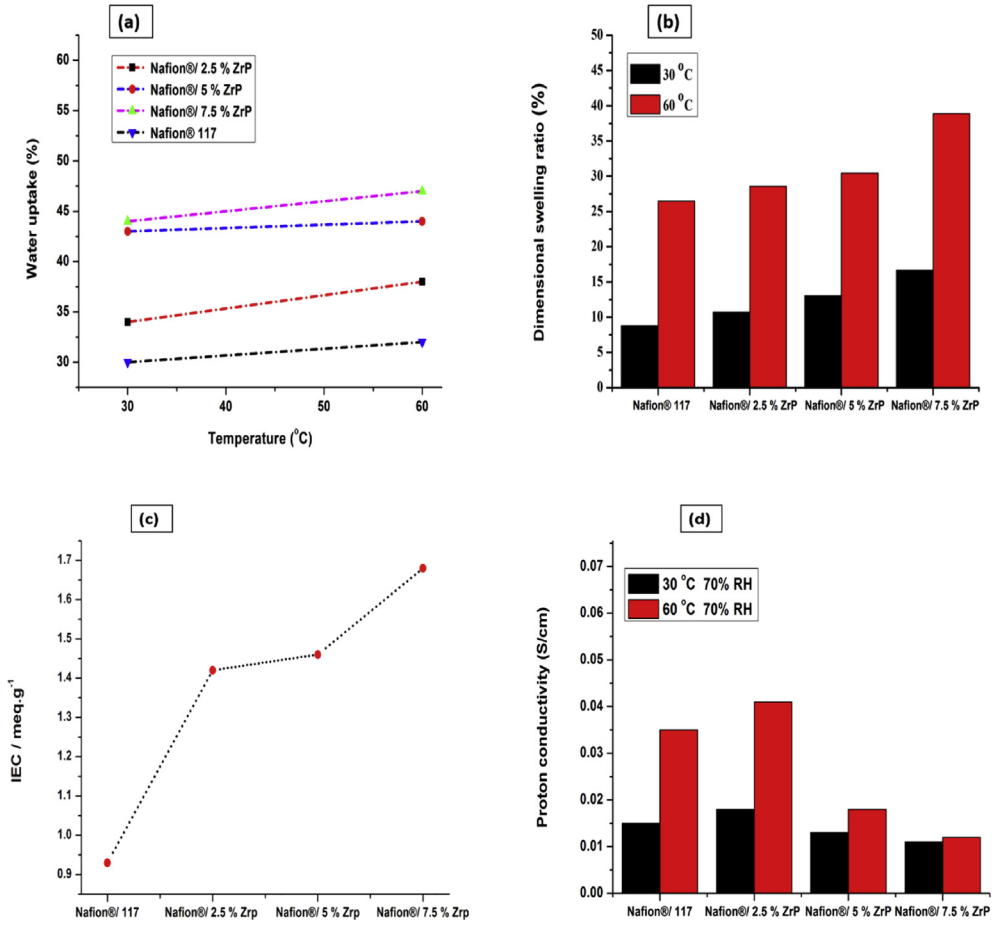

Fig. 7. Water uptake (a), linear expansion (b), Ion exchange capacity(c) and proton conductivity measurement (d) of Nafion® 117 membranes and Nafion®/2.5% ZrP, Nafion®/5% ZrP and Nafion®/7.5% ZrP nanocomposite membranes.

Table 2
The proton conductivity at 30 °C and 60 °C at 70% RH and IEC of Nafion® 117, Nafion®/2.5% ZrP, Nafion®/5% ZrP and Nafion®/7.5% ZrP nanocomposite membranes.

Membranes	Proton conductivity (S/cm) at 30 °C and 70% RH	Proton conductivity (S/cm) at 60 °C and 70% RH	IEC
Nafion® 117	0.015	0.035	0.93
Nafion®/2.5 % ZrP	0.018	0.041	1.42
Nafion®/5 % ZrP	0. 013	0.018	1.46
Nafion®/7.5 % ZrP	0.011	0.012	1.68

2.6. The Nafion®/2.5% ZrP, Nafion®/5% ZrP and Nafion®/7.5% ZrP nanocomposite membrane shows an increased in water-uptake (38 %, 44 % and 47 %) whereas the commercial Nafion® 117 membrane obtained the lower water uptake of 32% at 60 °C as indicated in Fig. 7(a). This may be due to incorporation of nanofillers that enhanced the hydrophilic of membranes [35]. Generally, when increases the ZrP loading within Nafion® 117 membranes, it also increases the water uptake, due to the hydrophilicity of adsorption acidic materials on the membrane surface to introduce the hydrophilicity and acidity of modified membrane surface [36]. The dimensional swelling ratio at 30 °C and 60 °C shows a slightly increased with the increases in wt% of ZrP nanoparticles within the membrane as shown in Fig. 7(b). However, when Nafion®/7.5% ZrP nanocomposite membrane was soaked at higher temperature of 60 °C, a higher dimensional swelling ratio of 39% was obtained. Moreover, when temperature increases also increases the dimensional stability and water uptake of the membranes.

The proton conductivity and Ion exchange capacity (IEC) of Nafion® 117 membrane, Nafion®/2.5% ZrP, Nafion®/5% ZrP and Nafion®/7.5% ZrP nanocomposite membranes are shown in Table 2 and Fig. 7(c & d). The results in Table 2 and Fig. 7(c) shows the IEC value of Nafion® 117, Nafion®/2.5% ZrP, Nafion®/5% ZrP and Nafion®/7.5% ZrP nanocomposite membranes are 0.93 meg. g^{-1}, 1.42 meg. g^{-1}, 1.46 meg. g^{-1} and 1.68 meg. g^{-1}, respectively. This may due to the impregnation of Nafion® membrane with ZrP, which provide the strong acid site within the membrane [36]. The IEC of the nanocomposites increases with the increases in wt% of ZrP nanoparticles within the membrane. Table 2 and Fig. 7 (d) shows that the proton conductivity of the Nafion®/7.5% ZrP and Nafion®/5% ZrP nanocomposite membranes (0.011 S cm^{-1} and 0.013 S cm^{-1}) at 30 °C were slightly lower than that of commercial Nafion® 117 membrane (0.015 S cm^{-1}) [37], this reduction in proton conductivity may be due to inorganic particles in the membranes. The results show that introducing the zirconia phosphate nanoparticles into the membrane decreases the proton conductivity at lower temperature [38]. Whereas the water uptake of the modified Nafion® membrane was higher than unmodified Nafion® membrane as shown in Fig. 7(a). The conductivity of Nafion®/2.5% ZrP nanocomposite membrane (0.041 S cm^{-1}) at 60 °C and 70% RH, found to be higher than the commercial Nafion® membrane (0.035 S cm^{-1}), due to the increases of temperature, which increases the conductivity while also lead to the dehydration of commercial membrane shown in Table 2 and Fig. 7(d) [35, 39].

3.8. Fuel cell performance

The power density and polarization curves were observed at 60 °C. The maximum power density of Nafion® 117 membrane, Nafion®/2.5% ZrP, Nafion®/5% ZrP and Nafion®/7.5% ZrP nanocomposite membranes were 126.04 mW cm^{-2}, 209.71 mW cm^{-2}, 206.79 mW cm^{-2} and 112.62 mW cm^{-2}, respectively. The Nafion®/2.5% ZrP and Nafion®/5% ZrP nanocomposite membranes obtained a higher power density than

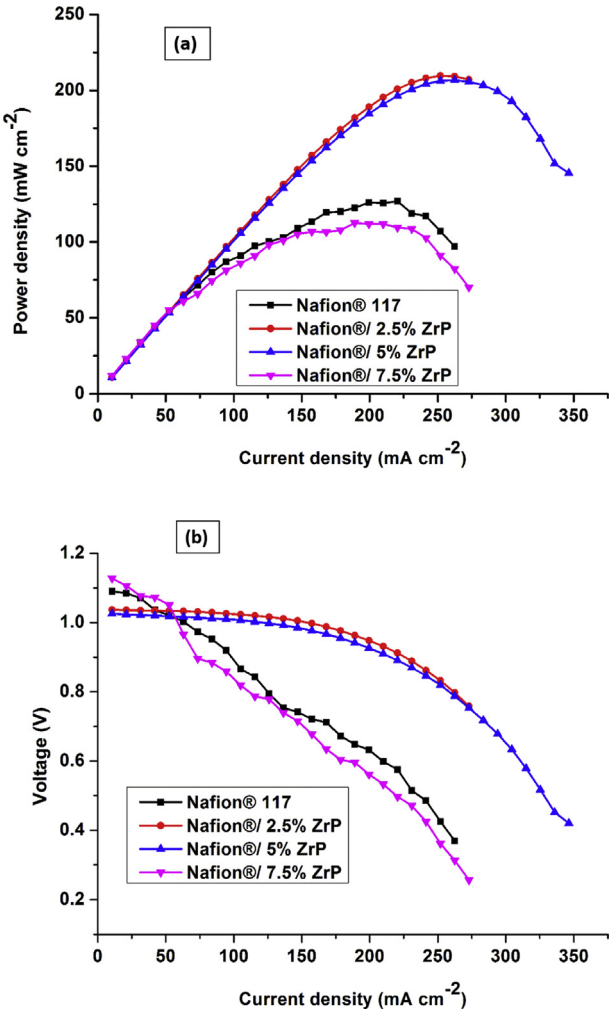

Fig. 8. (a &b) DMFC polarization of Nafion® 117 membrane, Nafion®/2.5% ZrP, Nafion®/5% ZrP and Nafion®/7.5% ZrP nanocomposite membranes obtained at 60 °C.

those of Nafion® 117 membrane. These may due to the ZrP nanoparticles incorporated within the Nafion® matrix that increases the efficiency of fuel cell at 60 °C. Furthermore, the power density increases may be due to the incorporation of ZrP that suppresses the ohmic resistance of the Nafion® membrane [40]. These higher DMFC performance also confirm by the higher conductivity of Nafion®/2.5% ZrP nanocomposite membrane at 60 °C. But the slightly decrease was obtained in the performance of Nafion®/7.5% ZrP nanocomposite membrane when compared to Nafion® 117 membrane, with the power density of 112.62 mW cm^{-2} and 126.04 mW cm^{-2} at the current densities of 189 mA cm^{-2}. The results show that when ZrP 7.5wt% impregnated within the membrane, as observed under TGA results resulted in agglomeration that hinders the cell performance. Therefore, Nafion® 117 membrane incorporated with 5% ZrP obtained the highest power density (145 mW cm^{-2}) than commercial membrane, with current density of 350 mA cm^{-2} as shown in Fig. 8(a). Fig. 8(b) show that the modified membrane obtained a higher voltage than commercial membrane. The Nafion®/7.5% ZrP nanocomposite membrane (0.50 V) also shows the slightly decreases in voltage at the current densities of 220 mA cm^{-2} when compared to Nafion® 117 membrane (0.58 V), Nafion®/2.5% ZrP (0.89 V) and Nafion®/5% ZrP (0.91 V) nanocomposite membranes. This may due to higher wt% of ZrP incorporated within the Nafion matrix membrane. The lower wt% incorporation shows the improvement in the voltage and current density. This may be due to the nanoparticles that well deposited

within the membrane pores, that are good in water retention and enhance the conductivity of modified membrane [41].

4. Conclusion

The preparation of the Nafion/ZrP nanocomposite membrane with low methanol permeability and good proton conductivity was successfully achieved by the impregnation method. The thermal stability of the nanocomposite membrane started to decompose at high temperature of 450 °C that may be due to the nature of an inorganic filler and their close interaction with the hydrophobic Nafion® backbones. Moreover, water uptake, IEC and linear expansion of nanocomposite membrane was enhanced compared to Nafion® 117 membrane at higher temperature of 60 °C. The results show the decrease of methanol permeability of modified Nafion® membrane at higher temperature of 80 °C and 5 M methanol concentration compared to Nafion® 117 membrane. The higher temperature conductivity on the nanocomposite membranes obtained an enhanced proton conductivity than commercial Nafion® membrane, due to the addition of inorganic materials within the membranes. The lower methanol permeation and high proton conductivity resistance of modified membrane also confirmed the suitability used in fuel cell. SEM and FTIR results confirm the incorporation ZrP in the membranes that also enhanced the water uptake. The Nafion®/2.5% ZrP (209.71 mW cm^{-2}) and Nafion®/5% ZrP (206.79 mW cm^{-2}) nanocomposite membranes obtained a higher power density than those of commercial Nafion® 117 membranes (126.04 mW cm^{-2}).

Declarations

Author contribution statement

Fulufhelo Nemavhola: Analyzed and interpreted the data; Contributed reagents, materials, analysis tools or data; Wrote the paper.

Rudzani Sigwadi: Conceived and designed the experiments; Performed the experiments; Analyzed and interpreted the data; Contributed reagents, materials, analysis tools or data; Wrote the paper.

Mokhotjwa Simon Dhlamini & Touhami Mokrani: Conceived and designed the experiments.

Patrick Nonjola & Phumlani Msomi: Performed the experiments.

Funding statement

This work was supported by the University of South Africa (AQIP) and The National research Foundation of South Africa (NRF).

Competing interest statement

The authors declare no conflict of interest.

Additional information

No additional information is available for this paper.

References

[1] K. Kreuer, Hydrocarbon membranes, Handb. Fuel Cells (2003).
[2] T.A. Zawodzinski, et al., Water uptake by and transport through Nafion® 117 membranes, J. Electrochem. Soc. 140 (4) (1993) 1041–1047.
[3] H. Yang, et al., Preparation of Nafion/various Pt-containing SiO 2 composite membranes sulfonated via different sources of sulfonic group and their application in self-humidifying PEMFC, J. Membr. Sci. 443 (2013) 210–218.
[4] C. Yang, Performance of Nafion/zirconium phosphate composite membranes in PEM fuel cells, Depart. Mech. Eng. (2003).
[5] F. Bauer, M. Willert-Porada, Characterisation of zirconium and titanium phosphates and direct methanol fuel cell (DMFC) performance of functionally graded Nafion (R) composite membranes prepared out of them, J. Power Sources 145 (2) (2005) 101–107.
[6] C. Yang, et al., Composite Nafion/zirconium phosphate membranes for direct methanol fuel cell operation at high temperature, Electrochem. Solid State Lett. 4 (4) (2001) A31–A34.
[7] G. Alberti, M. Casciola, Solid state protonic conductors, present main applications and future prospects, Solid State Ion. 145 (1) (2001) 3–16.
[8] M. Winter, J.O. Besenhard, Electrochemical lithiation of tin and tin-based intermetallics and composites, Electrochim. Acta 45 (1) (1999) 31–50.
[9] P. Costamagna, et al., Nafion® 115/zirconium phosphate composite membranes for operation of PEMFCs above 100 C, Electrochim. Acta 47 (7) (2002) 1023–1033.
[10] G. Alberti, et al., Novel Nafion–zirconium phosphate nanocomposite membranes with enhanced stability of proton conductivity at medium temperature and high relative humidity, Electrochim. Acta 52 (28) (2007) 8125–8132.
[11] F. Bauer, M. Willert-Porada, Microstructural characterization of Zr-phosphate–Nafion® membranes for direct methanol fuel cell (DMFC) applications, J. Membr. Sci. 233 (1) (2004) 141–149.
[12] C.,S.S. Yang, A.B. Bocarsly, S. Tulyani, J.B. Benziger, A comparison of physical properties and fuel cell performance of Nafion and zirconium phosphate/Nafion composite membranes, J. Membr. Sci. 237 (1-2) (2004) 145–161.
[13] G. Vaivars, et al., Zirconium phosphate based inorganic direct methanol fuel cell, Mater. Sci. 10 (2004) 162–165.
[14] V. Baglio, A. Di Blasi, V. Antonucci, FTIR spectroscopic investigation of inorganic fillers for composite DMFC membranes, Electrochem. Commun. 5 (10) (2003) 862–866.
[15] J. Ostrowska, A. Narebska, Infrared study of hydration and association of functional groups in a perfluorinated Nafion membrane, Part 1, Colloid Polym. Sci. 261 (2) (1983) 93–98.
[16] Y. Zhai, et al., Preparation and characterization of sulfated zirconia (SO42−/ZrO2)/Nafion composite membranes for PEMFC operation at high temperature/low humidity, J. Membr. Sci. 280 (1-2) (2006) 148–155.
[17] V. Di Noto, et al., Effect of SiO2 on relaxation phenomena and mechanism of ion conductivity of [Nafion/(SiO2) x] composite membranes, J. Phys. Chem. B 110 (49) (2006) 24972–24986.
[18] M. Laporta, M. Pegoraro, L. Zanderighi, Perfluorosulfonated membrane (Nafion): FT-IR study of the state of water with increasing humidity, Phys. Chem. Chem. Phys. 1 (19) (1999) 4619–4628.
[19] S. Horsley, D. Nowell, D. Stewart, The infrared and Raman spectra of α-zirconium phosphate, Spectrochim. Acta A Mol. Spectrosc 30 (2) (1974) 535–541.
[20] R. Pullar, M. Taylor, A. Bhattacharya, The manufacture of partially-stabilised and fully-stabilised zirconia fibres blow spun from an alkoxide derived aqueous sol–gel precursor, J. Eur. Ceram. Soc. 21 (1) (2001) 19–27.
[21] D. Sarkar, et al., Synthesis and characterization of sol–gel derived ZrO 2 doped Al 2 O 3 nanopowder, Ceram. Int. 33 (7) (2007) 1275–1282.
[22] M. Salavati-Niasari, M. Dadkhah, F. Davar, Pure cubic ZrO 2 nanoparticles by thermolysis of a new precursor, Polyhedron 28 (14) (2009) 3005–3009.
[23] H.W. Starkweather Jr., Crystallinity in perfluorosulfonic acid ionomers and related polymers, Macromolecules 15 (2) (1982) 320–323.
[24] K. Li, et al., Self-assembled Nafion®/metal oxide nanoparticles hybrid proton exchange membranes, J. Membr. Sci. 347 (1) (2010) 26–31.
[25] R. Sigwadi, et al., Mechanical strength of Nafion®/ZrO2 nano-composite membrane, Int. J. Manuf. Mater. Mech. Eng. 8 (1) (2018) 54–65.
[26] T. Kyu, M. Hashiyama, A. Eisenberg, Dynamic mechanical studies of partially ionized and neutralized Nafion polymers, Can. J. Chem. 61 (4) (1983) 680–687.
[27] B. Smitha, D.A. Devi, S. Sridhar, Proton-conducting composite membranes of chitosan and sulfonated polysulfone for fuel cell application, Int. J. Hydrogen Energy 33 (15) (2008) 4138–4146.
[28] Y. Devrim, et al., Improvement of PEMFC performance with Nafion/inorganic nanocomposite membrane electrode assembly prepared by ultrasonic coating technique, Int. J. Hydrogen Energy 37 (21) (2012) 16748–16758.
[29] Q. Deng, et al., TGA–FTi. r. investigation of the thermal degradation of Nafion® and Nafion®/[silicon oxide]-based nanocomposites, Polymer 39 (24) (1998) 5961–5972.
[30] Y. Wang, et al., Influence of polymeric binders on mechanical properties and microstructure evolution of silicon composite electrodes during electrochemical cycling, J. Power Sources 425 (2019) 170–178.
[31] Z. Lu, et al., An experimental investigation of strain rate, temperature and humidity effects on the mechanical behavior of a perfluorosulfonic acid membrane, J. Power Sources 214 (2012) 130–136.
[32] E. Safronova, et al., Sensitivity of potentiometric sensors based on Nafion®-type membranes and effect of the membranes mechanical, thermal, and hydrothermal treatments on the on their properties, Sens. Actuators B Chem. 240 (2017) 1016–1023.
[33] P. Xing, et al., Synthesis and characterization of poly (aryl ether ketone) copolymers containing (hexafluoroisopropylidene)-diphenol moiety as proton exchange membrane materials, Polymer 46 (10) (2005) 3257–3263.
[34] T. Yang, Composite membrane of sulfonated poly (ether ether ketone) and sulfated poly (vinyl alcohol) for use in direct methanol fuel cells, J. Membr. Sci. 342 (1) (2009) 221–226.

[35] S. Bose, et al., Polymer membranes for high temperature proton exchange membrane fuel cell: recent advances and challenges, Prog. Polym. Sci. 36 (6) (2011) 813–843.
[36] S. Peighambardoust, S. Rowshanzamir, M. Amjadi, Review of the proton exchange membranes for fuel cell applications, Int. J. Hydrogen Energy 35 (17) (2010) 9349–9384.
[37] L.S. Wang, et al., Orderly sandwich-shaped graphene oxide/Nafion composite membranes for direct methanol fuel cells, J. Membr. Sci. 492 (2015) 58–66.
[38] R. Sigwadi, Zirconia based/Nafion Coposite Membranes for Fuel Cell Applications, 2013.
[39] A. Ahmad, K.M. Isa, Z. Osman, Conductivity and structural studies of plasticized polyacrylonitrile (PAN)-lithium triflate polymer electrolyte films, Sains Malays. 40 (7) (2011) 691–694.
[40] H.-Y. Li, Y.-L. Liu, Nafion-functionalized electrospun poly (vinylidene fluoride)(PVDF) nanofibers for high performance proton exchange membranes in fuel cells, J. Mater. Chem. 2 (11) (2014) 3783–3793.
[41] G.G. Kumar, K.S. Nahm, Polymer nanocomposites-fuel cell applications, in: Advances in Nanocomposites-Synthesis, Characterization and Industrial Applications, IntechOpen, 2011.